

MULTIFUNCTIONAL IRON OXIDE SUPPORTED ALUMINA/YTTRIA
STABILIZED ZIRCONIA HOLLOW FIBER ADSORPTIVE MEMBRANE FOR
WATER TREATMENT

SYAFIKAH HUDA BINTI PAIMAN

UNIVERSITI TEKNOLOGI MALAYSIA

MULTIFUNCTIONAL IRON OXIDE SUPPORTED ALUMINA/YTTRIA-
STABILIZED ZIRCONIA HOLLOW FIBER ADSORPTIVE MEMBRANE FOR
WATER TREATMENT

SYAFIKAH HUDA BINTI PAIMAN

A thesis submitted in fulfilment of the
requirements for the award of the degree of
Doctor of Philosophy

School of Chemical and Energy Engineering
Faculty of Engineering
Universiti Teknologi Malaysia

NOVEMBER 2020

ACKNOWLEDGEMENT

Alhamdulillah. All praises Be to Allah, The Most Loving, The Most Merciful. To my parents (Paiman bin Sanusi and Rozi Noriah Binti Sukarno), my sister (Nurul Azwa), my brother (Mohd Rafiq) and all family members. Thank you for your unconditional love by believing in me, during critical periods of my life when I did not believe much in myself.

Sincerely thank you to my supervisor Assoc. Prof. Dr Mukhlis bin A Rahman for his guidance and endless support throughout my study. I felt very comfortable expressing my opinion at all times, and I am grateful to have benefited from your extensive experience and knowledge not only in academic life but also in many other aspects of life as a researcher and as a slave of Allah in general. Thank you to my research group members; Norfazliana, Dr Siti Nurfatin Nadhirah, Intan Nuralisa, Nur Zhatul Shima, Amirul, Nur Naziiha, Zahir, Nizar, Nor Fazilah and Nor Fadilah.

Special thanks to all members of Fine Particles Research Group at National Institute for Materials Science (NIMS), Japan; Prof. Dr. Tetsuo Uchikoshi, Dr. Ngan Kim Thi Nguen, and Dr. Ishii Kento for their help during my International Collaborative Graduate Program (ICGP) at NIMS (February 2018 – February 2019).

Infinite thanks to my dearest friends: Dr Nor Azureen, Dr Norfadhilatuladha, Faten Ermala, Nuridayu, Ts. Dr. Nur Hashimah and Dr. Nik Abdul Hadi, who showed me care, support and inspired me by exemplifying love through your selflessness, and generosity.

Also, thanks to all member of Advanced Membrane Technology Research Centre for the help I have received. I only ask that Allah bless you with His incredible goodness in ways that only He can. Lastly, I am grateful to the Ministry of Science, Technology and Innovation (MOSTI) and Universiti Teknologi Malaysia (UTM) for the financial supports.

ABSTRACT

Ceramic membrane offers high thermal, mechanical and chemical resistance. It also has been regarded as an alternative membrane for water separation application. In this study, a composite aluminium oxide/yttria-stabilized zirconia ($\text{Al}_2\text{O}_3/\text{YSZ}$) hollow fiber membrane was fabricated via the combined dry-wet phase inversion spinning method and sintering process. The findings had observed an asymmetrical membrane structure consisting of the finger-like voids and sponge-like voids. The addition of YSZ had improved the mechanical strength of the membrane produced despite the porous structure and thin wall thickness. The findings had concluded that the $\text{Al}_2\text{O}_3/\text{YSZ}$ hollow fiber membrane prepared using the composite of $0.3 \mu\text{m}$ YSZ particle and sintered at 1350°C (HF0.3-1350 membrane) was selected as the substrate for iron oxide (Fe_2O_3) deposition. This is due to the HF0.3-1350 measured to be having the highest water flux. Next, the deposition of Fe_2O_3 on the $\text{Al}_2\text{O}_3/\text{YSZ}$ hollow fiber membrane was carried out using the hydrothermal process. The hydrothermal process is a facile process and the Fe_2O_3 particles can be simultaneously synthesized and deposited. For the application of an adsorptive membrane for lead (Pb) removal, the Fe_2O_3 particles were deposited onto the porous structure of the membrane. The performance showed high Pb (II) removal at pH 7, with fast removal within the first 10 min of the filtration process and had reached the equilibrium at 60 min. Moreover, the kinetic isotherm of pristine, F005-24 and F02-24 membrane followed the pseudo-second-order kinetics model. This study proved that the Fe_2O_3 deposition played an indispensable role in improving the adsorption capability of the pristine membrane towards Pb (II) ions. For the application of oil emulsion separation, the Fe_2O_3 particles were deposited on the outer surface of the $\text{Al}_2\text{O}_3/\text{YSZ}$ hollow fiber membrane. Then, depositing at the hydrothermal concentration above 0.2 M, Fe_2O_3 layer was formed. The findings have shown that the Fe_2O_3 layer gave increment to the water flux and oil rejection of the membrane. Then, the property of Fe_2O_3 itself as a photocatalyst gave other functionalities of the membrane for the photocatalytic process. Therein, the stimulated photo-induced separation system was operated for the Fe_2O_3 supported $\text{Al}_2\text{O}_3/\text{YSZ}$ hollow fiber membrane to highlight the self-cleaning mechanism of the membrane. The finding recorded was that the flux and oil rejection increases with the light assisted throughout the separation process. Lastly, the polymer coating of UV curable resin (UVR) on the outer membrane surface had preserved the Fe_2O_3 layer from the delamination. The UVR layer formed had changed the surface properties of the membrane from hydrophilic to hydrophobic. The existence of the UVR layer had highlighted the potential of the hydrophobic UVR-coated ceramic hollow fiber membrane for water separation using the sweeping liquid filtration system. The F02-UVR membrane was able to remove 94% of humic acid with a flux of $46.53 \text{ kg/m}^2\cdot\text{h}$. The outcome of this study was the multifunctional Fe_2O_3 supported $\text{Al}_2\text{O}_3/\text{YSZ}$ hollow fiber adsorptive membrane can be used for the treatment of different water pollutant.

ABSTRAK

Membran seramik telah menawarkan rintangan terma, mekanik dan kimia yang tinggi. Membran ini juga telah dianggap sebagai membran alternatif untuk aplikasi pemisahan air. Kajian ini membran gentian berongga alumina/yttria-stabil zirkonia ($\text{Al}_2\text{O}_3/\text{YSZ}$) komposit dibuat melalui gabungan teknik pemejaman kering-basah dan proses pensinteran. Pemerhatian terhadap hasil kajian mendapati membran yang terhasil mempunyai struktur yang terdiri dari lompong seperti jari dan lompong seperti span. Kajian juga mendapati campuran partikel YSZ telah berjaya meningkatkan kekuatan mekanikal membran walaupun struktur membran yang terhasil mempunyai ketebalan dinding yang nipis dan berongga. Hasil kajian merumuskan bahawa membran gentian berongga $\text{Al}_2\text{O}_3/\text{YSZ}$ yang dihasilkan menggunakan campuran partikel YSZ bersaiz $0.3 \mu\text{m}$ dan disinter pada suhu 1350°C (HF0.3-1350) telah dipilih untuk digunakan sebagai substrat untuk pemendapan ferik oksida (Fe_2O_3). Hal ini kerana membran HF0.3-1350 merekodkan fluks air yang paling tinggi. Seterusnya, pemendapan ferik oksida (Fe_2O_3) di atas membran gentian berongga $\text{Al}_2\text{O}_3/\text{YSZ}$ dilakukan dengan menggunakan proses hidroterma. Proses ini mudah dan membolehkan penghasilan dan pemendapan partikel Fe_2O_3 dijalankan secara serentak. Untuk penggunaan membran sebagai membran penjerap untuk penyingkiran plumbum (Pb), partikel Fe_2O_3 dimendapkan di dalam membran gentian berongga $\text{Al}_2\text{O}_3/\text{YSZ}$. Prestasi membran mencatatkan penyingkiran Pb (II) yang tinggi dan cepat pada pH 7 dalam masa 10 minit pertama proses pemisahan dan mencapai keseimbangan pada minit ke-60. Tambahan lagi, kinetik isoterma bagi membran kosong, membran F005-24 dan membran F02-24 telah mengikuti model kinetik pseudo-tertib kedua. Kajian ini juga membuktikan bahawa pemendapan Fe_2O_3 memainkan peranan dalam meningkatkan kebolehpayaan membran kosong untuk proses penjerapan ion Pb (II). Untuk aplikasi membran bagi tujuan pemisahan emulsi minyak, partikel Fe_2O_3 telah dimendapkan di atas permukaan luar membran gentian berongga $\text{Al}_2\text{O}_3/\text{YSZ}$. Proses pemendapan menggunakan cecair hidroterma dengan kelikatan di atas 0.2 M telah menghasilkan lapisan Fe_2O_3 . Hasil kajian mendapati kehadiran lapisan Fe_2O_3 telah meningkatkan fluks air dan penyingkiran minyak oleh membran. Kemudian, sifat partikel Fe_2O_3 sebagai fotomangkin telah memberikan fungsi baharu kepada membran untuk proses foto pemangkinan. Justeru, sistem pemisahan dengan rangsangan cahaya telah dikendalikan untuk membran gentian berongga $\text{Al}_2\text{O}_3/\text{YSZ}$ yang menyokong Fe_2O_3 untuk menonjolkan fungsi kebolehan pembersihan-sendiri oleh membran. Hasil kajian menunjukkan peningkatan terhadap fluks dan penyingkiran minyak dengan kehadiran cahaya di sepanjang proses pemisahan berlaku. Akhir sekali, salutan polimer resin UV yang boleh diubah (UVR) di atas permukaan luar membran telah memelihara lapisan Fe_2O_3 daripada tanggal. Selain itu, lapisan UVR juga telah mengubah sifat membran daripada hidrofilik kepada hidrofobik. Kehadiran lapisan UVR telah menonjolkan keupayaan membran gentian berongga seramik hidrofobik untuk proses pemisahan air menggunakan sistem pemisahan sapuan cecair. Membran F02-UVR berjaya menyingkirkan 94% asid humik dengan jumlah fluks $46.53 \text{ kg/m}^2 \cdot \text{h}$. Kajian mendapati penjerapan membran multifungsi Fe_2O_3 yang disokong di atas gentian berongga $\text{Al}_2\text{O}_3/\text{YSZ}$ boleh digunakan untuk merawat pencemar air yang berbeza.

TABLE OF CONTENT

	TITLE	PAGE
	DECLARATION	iii
	DEDICATION	iv
	ACKNOWLEDGEMENT	v
	ABSTRACT	vi
	ABSTRAK	vii
	TABLE OF CONTENT	viii
	LIST OF TABLES	xii
	LIST OF FIGURES	xiv
	LIST OF ABBREVIATIONS	xviii
	LIST OF SYMBOLS	xx
	LIST OF APPENDICES	xxii
CHAPTER 1	INTRODUCTION	1
1.1	Research Background	1
1.2	Problem Background	2
1.3	Objectives	5
1.4	Scope of the Study	5
1.5	Significant of Study	8
CHAPTER 2	LITERATURE REVIEW	11
2.1	Ceramic Membrane	11
2.2	Fabrication of an Asymmetric Ceramic Hollow Fiber Membrane	12
2.2.1	Composite Ceramic Membrane	20
2.3	Adsorptive Ceramic Hollow Fiber Membrane	26
2.3.1	Application for Heavy Metal Removal	28
2.4	Photocatalytic Ceramic Hollow Fiber Membrane	33
2.4.1	Application for Oil Emulsion Separation	37

2.5	Ceramic Hollow Fiber Membrane for Humic Acid Removal	40
2.6	Iron Oxide for Water Remediations (Adsorptive Removal and Photocatalytic Degradation)	40
2.6.1	Hydrothermal Synthesis Methods for Iron Oxide	48
CHAPTER 3	RESEARCH METHODOLOGY	55
3.1	Introduction	55
3.2	Materials	58
3.2.1	For Substrate	58
3.2.2	For In-situ Hydrothermal Deposition	58
3.2.3	For Polymer Coating	58
3.3	Fabrication of Al ₂ O ₃ /YSZ Hollow Fiber Membrane as Substrate	59
3.3.1	Suspension Preparation	59
3.3.2	Spinning	61
3.3.3	Sintering	63
3.4	In-situ Hydrothermal Deposition of Iron Oxide	64
3.5	UV Curable Resin Coating	67
3.6	Characterizations	68
3.6.1	Scanning Electron Microscopy (SEM)	68
3.6.2	Field Emission Electron Microscopy (FESEM)	68
3.6.3	Atomic Force Microscopy (AFM)	69
3.6.4	Mercury Intrusion Porosimetry	69
3.6.5	Three-Point (3P) Bending Strength	70
3.6.6	X-Ray Diffraction (XRD)	71
3.6.7	Pure Water Permeation	71
3.7	Adsorptive Membrane Study for Lead (Pb) Removal	73
3.7.1	Adsorption Isotherms and Kinetics	74
3.8	Oil Emulsion Separation	75
3.8.1	The Oil Emulsion Separation with the Light Assisted Filtration System	76
3.9	Sweeping Liquid Crossflow Filtration Study for Humic Acid	79

CHAPTER 4	RESULTS AND DISCUSSIONS	83
4.1	Fabrication of Alumina Oxide/Yttria-Stabilized Zirconia ($\text{Al}_2\text{O}_3/\text{YSZ}$) Hollow Fiber Membrane	83
4.1.1	The Structural properties of $\text{Al}_2\text{O}_3/\text{YSZ}$ Hollow Fiber Membrane	83
4.1.2	The Physical Properties of $\text{Al}_2\text{O}_3/\text{YSZ}$ Hollow Fiber Membrane	87
4.1.3	Remarks	89
4.2	Hydrothermal Deposition of Iron Oxide (Fe_2O_3) across the $\text{Al}_2\text{O}_3/\text{YSZ}$ Hollow Fiber Membrane for Lead (Pb) Removal	90
4.2.1	Structural Properties	90
4.2.2	X-Ray Diffractogram (XRD) Pattern	92
4.2.3	N_2 Adsorption-Desorption	95
4.2.4	The Permeation of Pure Water	97
4.2.5	Adsorptive Membrane Study on Pb (II) Ions Removal	98
4.2.5.1	The Effect of pH Value of Pb (II) Solution	98
4.2.5.2	The Effect of Time Contact and Adsorption Kinetics	100
4.2.5.3	Mechanism of Adsorptive Membrane	102
4.2.6	Remarks	104
4.3	Hydrothermal Deposition of Fe_2O_3 on the Outer Surface of the $\text{Al}_2\text{O}_3/\text{YSZ}$ Hollow Fiber Membrane for Oil Emulsion Separation	105
4.3.1	Structural Properties of Fe_2O_3 Supported $\text{Al}_2\text{O}_3/\text{YSZ}$ Hollow Fiber Membrane	105
4.3.2	The Physical Properties of the Fe_2O_3 Supported Membrane and Fe_2O_3 Particles	109
4.3.3	The permeation of Pure Water	114
4.3.4	The Performance for Oil Emulsion Separation	115
4.3.5	Photodegradation of Oil Emulsion	118
4.3.6	The Stimulated Photo-Induced Separation of Oil Emulsion	120
4.3.7	Remarks	123

4.4	The Feasibility of Fe ₂ O ₃ Supported Al ₂ O ₃ /YSZ Hollow Fiber Membrane for Sweeping Liquid Filtration Process	124
4.4.1	Structural Properties of Membrane with UV Curable Resin Coating	124
4.4.2	Physicochemical Properties of UV Curable Resin Coating	127
4.4.3	The Performance for Humic Acid Removal	130
4.4.4	Remarks	133
CHAPTER 5	CONCLUSION AND RECOMMENDATIONS	135
5.1	Conclusions	135
5.2	Recommendations	137
	REFERENCES	139
	APPENDICES	159
	LIST OF PUBLICATIONS	161

LIST OF TABLES

TABLE NO.	TITLE	PAGE
Table 2.1	The fabrication steps of ceramic hollow fiber membrane including the remarks.	19
Table 2.2	List of composite ceramic hollow fiber membrane, composite materials, composite technique and the remarks.	24
Table 2.3	The list of heavy metal ions, effects and the maximum concentration level in the water.	29
Table 2.4	List of adsorptive ceramic hollow fiber membrane for heavy metal removal.	32
Table 2.5	List and summary of photocatalytic ceramic membrane.	36
Table 2.6	List of hydrophilic coating on ceramic membrane for oily wastewater treatment.	39
Table 2.7	List of iron-based oxide particles for adsorption of heavy metal ions.	44
Table 2.8	List of iron-based oxide particles as a photocatalyst.	46
Table 2.9	The operational condition of the hydrothermal synthesis method for iron oxide.	52
Table 3.1	The composition of the ceramic suspension.	60
Table 3.2	The spinning conditions for the fabrication of the Al ₂ O ₃ /YSZ hollow fiber membrane.	63
Table 3.3	Sample designation of the Al ₂ O ₃ /YSZ hollow fiber prepared at different YSZ particles sizes and sintering temperature.	64
Table 3.4	The in-situ hydrothermal conditions for depositing Fe ₂ O ₃ in the inner region (across the membrane structure) of the Al ₂ O ₃ /YSZ hollow fiber membrane.	65
Table 3.5	The in-situ hydrothermal conditions for depositing Fe ₂ O ₃ on the surface of the Al ₂ O ₃ /YSZ hollow fiber membrane.	66
Table 3.6	Sample designation of the hollow fiber membrane coated with UV curable resin.	67
Table 4.1	The wall thickness of the Al ₂ O ₃ /YSZ hollow fiber membrane at different sintering temperatures and YSZ particle sizes.	87

Table 4.2	The mechanical strength and water flux of Al ₂ O ₃ /YSZ hollow fiber membrane sintered at different sintering temperatures and YSZ particle sizes.	89
Table 4.3	The average crystallite size of Fe ₂ O ₃ .	94
Table 4.4	N ₂ adsorption-desorption analysis data for Fe ₂ O ₃ particles prepared at different hydrothermal concentration and duration.	95
Table 4.5	Kinetics first-order and second-order parameters for Pb (II) ions adsorption on pristine Al ₂ O ₃ /YSZ membrane and deposited Fe ₂ O ₃ membrane.	102
Table 4.6	The contact angle value and the apparent porosity of pristine Al ₂ O ₃ /YSZ hollow fiber membrane and Fe ₂ O ₃ supported Al ₂ O ₃ /YSZ hollow fiber membrane.	110
Table 4.7	The N ₂ adsorption-desorption analysis data for Fe ₂ O ₃ particles prepared at different hydrothermal concentration. 0.05 M – F005, 0.2 M – F02 and 0.5 M – F05.	112
Table 4.8	The Fe ₂ O ₃ particle loading on Al ₂ O ₃ /YSZ hollow fiber membrane.	119
Table 4.9	The zeta potential values of oil emulsion and Fe ₂ O ₃ particles.	120
Table 4.10	The water flux, solute flux and solute rejection membranes using a pressure-driven system of 1000 mg/L of humic acid solution.	131
Table 4.11	Sweeping liquid filtration of 1000 mg/L of humic acid solution.	132

LIST OF FIGURES

FIGURE NO.	TITLE	PAGE
Figure 2.1	The illustration of the separation process for the ceramic membrane.	11
Figure 2.2	The illustration of an asymmetric ceramic membrane.	12
Figure 2.3	The illustration of increasing membrane packing density at different particle size distribution.	13
Figure 2.4	Cross-sectional images of Al ₂ O ₃ hollow fiber membrane prepared at the varying amount of water in the ceramic suspension made [10].	14
Figure 2.5	The structure of Al ₂ O ₃ hollow fiber membrane fabricated; a) without air-gap and b) with air-gap in a length of 20 cm.	16
Figure 2.6	The sintering stage of the sintering process to fabricate ceramic membrane.	17
Figure 2.7	The schematic process of dextran separation using pristine membrane and the ZrO ₂ nanoporous membrane.	21
Figure 2.8	Membrane/adsorbent combination modes in respect of adsorptive ceramic membrane concept. (a) the adsorbent is dispersed in the tank of heavy metal ions solution, (b) adsorbent is deposited across the porous membrane and (c) adsorbent is deposited on top of the membrane surface.	28
Figure 2.9	The illustration of adsorptive-separative ceramic hollow fiber process.	31
Figure 2.10	The illustration of the photocatalytic activity of a photocatalyst.	34
Figure 2.11	Mechanism of the self-cleaning membrane surface.	35
Figure 2.12	The illustration of electrostatic repulsion and attraction of oil droplets to the ceramic membrane for oily wastewater separation.	38
Figure 2.13	The α -Fe ₂ O ₃ structural evolution using a different type of solvent in the hydrothermal synthesis method [142].	49
Figure 2.14	The illustration of templated-assisted; a) soft-templated and b) hard-templated for porous iron oxide formation [153].	51
Figure 3.1	The flow chart of the research study.	57

Figure 3.2	The illustration steps for the preparation of the ceramic suspension.	60
Figure 3.3	The illustration of the degassing system for ceramic suspension.	61
Figure 3.4	The illustration of the spinning system for the fabrication of the Al ₂ O ₃ /YSZ hollow fiber membrane.	62
Figure 3.5	The sintering temperature profile.	64
Figure 3.6	The illustration of the in-situ hydrothermal process of iron oxide on the inner surface and outer surface of the Al ₂ O ₃ /YSZ hollow fiber membrane. (a) hydrothermal synthesis step, and (b) calcination.	66
Figure 3.7	The illustration of UV curable resin coating under UV treatment for powder form and membranes.	67
Figure 3.8	The illustration for the 3P bending strength test of the hollow fiber membrane.	70
Figure 3.9	The schematic diagram of the crossflow filtration system.	72
Figure 3.10	a) Membrane module for visible light assisted filtration process in cross-flow configuration and b) the union cross-module assembled for the membrane.	78
Figure 3.11	The schematic of a photocatalytic process for oil emulsion in the batch process.	78
Figure 3.12	The schematic configuration of a sweeping liquid crossflow filtration system for humic acid removal.	81
Figure 4.1	The SEM images of Al ₂ O ₃ /YSZ hollow fiber membrane sintered at different sintering temperatures for 6 h. a) HF0.3-1350, b) HF0.3-1400, c) HF0.01-1350, d) HF0.01-1400; i) overall morphology, ii) cross-sectional structure and iii) the outer surface of the membrane.	85
Figure 4.2	The EDX images of HF0.3-1350 membrane; (a) the cross-sectional and (b) the outer surface.	86
Figure 4.3	Mercury intrusion porosimetry of the Al ₂ O ₃ /YSZ hollow fiber membrane at a different YSZ particle size and sintering temperature.	88
Figure 4.4	The FESEM images of the cross-sectional and outer surface of Fe ₂ O ₃ supported Al ₂ O ₃ /YSZ hollow fiber membrane at different hydrothermal concentration and hydrothermal duration. (a) F005-24, (b) F005-48, (c) F02-24 and (d) F02-48.	91
Figure 4.5	The FESEM-EDX spectrum for the F02-24 membrane.	92

Figure 4.6	(a) XRD diffractograms of pristine Al ₂ O ₃ /YSZ hollow fiber, Fe ₂ O ₃ supported Al ₂ O ₃ /YSZ hollow fiber (F02-24 membrane) and Fe ₂ O ₃ particles (F02-24 particles). (b) close-up XRD diffractogram at range 32° to 34°.	93
Figure 4.7	XRD diffractogram of collected Fe ₂ O ₃ particles synthesized at different hydrothermal concentration and hydrothermal duration.	94
Figure 4.8	The illustration of the mesoporous structure of Fe ₂ O ₃ formation via hydrothermal-soft template-assisted.	96
Figure 4.9	Water flux of pristine and supported Fe ₂ O ₃ across the Al ₂ O ₃ /YSZ hollow fiber membrane at different in-situ hydrothermal process conditions.	97
Figure 4.10	The effect of pH value of Pb (II) solution on the removal Pb (II) ions; (a) using membranes and (b) using Fe ₂ O ₃ particles and (c) the zeta potential of Fe ₂ O ₃ F02-24 particles.	99
Figure 4.11	a) Adsorptive membrane cumulative permeate, percentage of Pb (II) removal, and c) the adsorption capacity for Pb (II) ions using 1 mg/L of Pb (II) solution at pH 7 at a different contact time.	101
Figure 4.12	The conceptual of the adsorptive ceramic hollow fibre membrane.	103
Figure 4.13	The structural images of (i) outer surface and (ii) cross section of pristine and deposited porous α-Fe ₂ O ₃ on Al ₂ O ₃ /YSZ HF membrane at different concentration; (a) 0.05 M (F005), (b) 0.2 M (F02), and (c) 0.5 M (F05).	107
Figure 4.14	FESEM images of Fe ₂ O ₃ particles at different iron precursor concentration; (a) 0.05 M, (b) 0.2 M and (c) 0.5 M.	108
Figure 4.15	The AFM images of (a) pristine membrane and Fe ₂ O ₃ supported membrane; (b) F005, (c) F02 and (d) F05.	109
Figure 4.16	N ₂ adsorption-desorption isotherms for Fe ₂ O ₃ particles prepared at different hydrothermal concentration. (a) 0.05 M – F005, (b) 0.2 M – F02 and (c) 0.5 M – F05.	111
Figure 4.17	The diffractogram of XRD analysis for Fe ₂ O ₃ particles prepared at different hydrothermal concentration.	113
Figure 4.18	(a) The FTIR spectra of Fe ₂ O ₃ particles (– F005, – F02 and – F05), (b) the spectra at a wavelength between 3100 – 3800 cm ⁻¹ , (c) the spectra at a wavelength between 1700 – 1500 cm ⁻¹ and (d) the spectra at a wavelength between 620 – 440 cm ⁻¹ .	114

Figure 4.19	The water flux of pristine and Fe ₂ O ₃ supported Al ₂ O ₃ /YSZ hollow fiber membrane.	115
Figure 4.20	The flux and rejection of 1000 mg/L oil emulsion using pristine Al ₂ O ₃ /YSZ hollow fiber membrane and Fe ₂ O ₃ supported Al ₂ O ₃ /YSZ hollow fiber membrane (F005, F02, and F05 membrane).	116
Figure 4.21	The size distribution of oil emulsion droplets at feed solution, at permeate for pristine membrane and permeate for F02 membrane.	118
Figure 4.22	Oil emulsion degradation under visible light irradiation for (●) pristine, (●) F005 HF, (●) F02 HF, and (●) F05 HF membranes. (●) The photolysis of oil emulsion degradation.	120
Figure 4.23	The Effect of calcination temperature and the on-line photo-induced self-cleaning. (■) without light irradiation and (▨) with light irradiation.	122
Figure 4.24	The conceptual of the self-cleaning membrane for oil emulsion separation.	122
Figure 4.25	FESEM images of a) pristine Al ₂ O ₃ /YSZ hollow fiber membrane and b) the Fe ₂ O ₃ supported membrane (F02 membrane); before and after coating with UV curable resin.	125
Figure 4.26	The AFM images of (a) pristine Al ₂ O ₃ /YSZ hollow fiber membrane and (b) the Fe ₂ O ₃ supported membrane; before and after coating with UV curable resin.	126
Figure 4.27	Fe ₂ O ₃ supported Al ₂ O ₃ /YSZ hollow fiber membrane (F02) with and without the UVR coating, and after being sonicated in water for 10 min.	127
Figure 4.28	FTIR spectra for UV curable resin, Fe ₂ O ₃ particles, and pristine Al ₂ O ₃ /YSZ hollow fiber before and after coating with UV curable resin.	128
Figure 4.29	XRD diffractogram of (a) Al ₂ O ₃ /YSZ and (b) Fe ₂ O ₃ ; (—) before and (---) after coating with UV curable resin.	129
Figure 4.30	The contact angle image and value of (a) pristine Al ₂ O ₃ /YSZ hollow fiber membrane and (b) the Fe ₂ O ₃ supported membrane (F02 membrane); before and after coating with UVR.	130

LIST OF ABBREVIATIONS

AA	-	Acetic acid
Al ₂ O ₃	-	Aluminium oxide
As	-	Arsenic
Cd	-	Cadmium
COOH	-	Carboxyl
CeO ₂	-	Cerium dioxide
CTAB	-	Cetyltrimethylammonium bromide
Cr	-	Chromium
Cu	-	Copper
CuO	-	Copper oxide
EDX	-	Energy dispersive x-ray spectroscopy
EtOH	-	Ethanol
EA	-	Ethanol amine
ED	-	Ethylene diamine
EG	-	Ethylene glycol
FESEM	-	Field emission electron microscopy
FTIR	-	Fourier transform infrared spectroscopy
HA	-	Humic acid
HCl	-	Hydrochloric acid
OH	-	Hydroxyl
Fe ₂ O ₃	-	Iron oxide
Pb	-	Lead
MCL	-	Maximum concentration level
MD	-	Membrane distillation
Hg	-	Mercury
MOF	-	Metal organic framework
MF	-	Microfiltration
MoS ₂	-	Molybdenum disulphide
MWCO	-	Molecular weight cut-off
NF	-	Nanofiltration

Ni	-	Nickel
NiO	-	Nickel oxide
NMP	-	N-Methylpyrrolidone
NMR	-	Nuclear magnetic resonance
PESf	-	Polyethersulfone
PTFE	-	Polytetrafluoroethylene
RO	-	Reverse osmosis
SEM	-	Scanning electron microscopy
NaOH	-	Sodium hydroxide
TiO ₂	-	Titanium dioxide
UF	-	Ultrafiltration
UV	-	Ultraviolet
UVR	-	UV curable resin
H ₂ O	-	Water
WHO	-	World Health Organization
XRD	-	X-ray diffraction
YSZ	-	Yttria-stabilized zirconia
Zn	-	Zinc

LIST OF SYMBOLS

A	-	Area of hollow fiber membrane
nm	-	Nanometre
μm	-	Micrometre
cm	-	Centimetre
mm	-	Millimetre
m	-	Meter
t	-	Time
s	-	Second
min	-	Minute
h	-	Hour
g	-	Gram
wt	-	Weight
T	-	Temperature
$^{\circ}\text{C}$	-	Degree Celsius
Pa.s	-	Viscosity
W	-	Watt
D_i	-	Inner diameter
D_o	-	Outer diameter
D_{cry}	-	Crystallite size
kN	-	Kilo newton
%	-	Percentage
θ	-	Degree
λ	-	Wavelength
M	-	Molar concentration
B_F	-	3P bending strength
F_M	-	Maximum load at which the fracture occurs
L_h	-	Span length
J_w	-	Flux
V	-	Volume
qt	-	Adsorption capacity at time

q_m	-	Adsorption capacity at equilibrium
C_i	-	Concentration at initial
C_f	-	Concentration at final
C_e	-	Concentration at equilibrium
C_p	-	Concentration at permeate
W_g	-	Weight of adsorbent
W_{HF}	-	Weight of membrane
$\Delta W_{M,feed}$	-	Weight change
W_D	-	Weight of dry membrane
W_S	-	Weight of suspended saturated membrane
W_{SS}	-	Weight of saturated membrane
R	-	Percentage rejection

LIST OF APPENDICES

APPENDIX	TITLE	PAGE
Appendix A	The measuring steps for apparent porosity of the hollow fiber membrane	159
Appendix B	The chemical structure of UV curable resin used in this study from the NMR analysis	160

CHAPTER 1

INTRODUCTION

1.1 Research Background

The global issue on the water scarcity is driven by the growth of the human population. The necessity and the increasing demand for high-quality water supply rise from the fact of the contaminated water caused by the human activities that are responsible for such a drastic decrease in water quality. Human activities such as in the industrial process, in the agricultural sector and daily activities with the improper disposal of waste material has been the major anthropogenic sources of the water contaminants. The contaminants such as heavy metal ions, organic compounds and natural organic compounds which having the excess into the food chains can cause to the waterborne illness. Hence, treating the contaminated water before safely channeled for consumption is primely important to protect environmental safety, aquatic life and human's health from intoxication.

Numbers of research study had introduced methods to treat the contaminated water that meets with the strict water quality standard. Such methods are the adsorption, separation and photocatalytic process. The adsorption process is an attractive method and widely used to remove water contaminants such as heavy metal ions due to its low cost, the availability of different adsorbents and simple operation. The photocatalytic process having the ability to decompose the organic water pollutants and enhanced the water quality. Then, the rising membrane technology had gathered a wide interest as an alternative method for water separation. The interesting part of membrane technology is that the advanced membranes can be fabricated with stimuli-responsive either by depositing the responsive materials into the membrane. These responsive materials, such as adsorbent and photocatalyst, to respond to the adsorption and photocatalytic process, respectively. The material deposition also response to the physical changes of the membrane properties, such as

pore size of the membranes, hydrophilicity and surface roughness. Therefore, the advanced membranes are capable of bringing a mammoth change and opportunities as a multifunctional membrane for water treatment.

In membrane technology, the development of the ceramic membrane has been extensively studied over the past few years due to the properties of the ceramic membrane that can overcome the limitation in the polymeric membrane [1]. The ceramic membrane is having a high resistance to high-temperature operation, high pressure and harsh chemical conditions. These properties are benefited to the ceramic membrane recovery to allow for the physical and chemical cleaning process [2,3]. Besides, the ceramic membrane is also having a lower fouling effect as compared to the polymeric membrane due to the hydrophilic properties of ceramic material [4]. In this study, a multifunctional ceramic hollow fiber membrane is highlighted. The membrane offers water separation for a different type of contaminants removal. As an adsorptive ceramic hollow fiber membrane, the membrane is beneficial for the removal of even low-concentration of heavy metal ions from aqueous water. Thus, the membrane can be a wise choice to replace the adsorbents in powder form for the adsorption process. Then, the photocatalytic process of the membrane is beneficial to reduce the membrane fouling effect by the degradation of organic pollutants. Thus, self-cleaning of the membrane surface membrane for oil emulsion separation can be done. Overall, the multifunctional properties of the membrane can assure plant simplicity.

1.2 Problem Background

Phase inversion technique is reported mostly in fabricating the ceramic hollow fiber membrane with a porous asymmetrical structure. The porous asymmetrical structure consisting of the sponge-like, and finger-like pores is favorable for a high flux membrane. The development of the combined alumina and YSZ particles for the ceramic hollow fiber membrane is not extensively studied yet. The phase inversion condition to achieve the desired membrane morphology is interesting to be studied. However, the concern related to the fabrication of ceramic hollow fiber membrane is

the membrane pore sizes produced. It was reported that the ceramic membranes produced via the phase inversion technique are having large membrane pore sizes. Normally in microfiltration (MF) and ultrafiltration (UF) range. The pore size of the ceramic membrane can be reduced to a nanofiltration (NF) or reverse osmosis (RO) range through the sintering process by increasing the sintering temperature. However, the densification of the sponge-like voids as prone to the sintering process leading to a formation of dense membrane structure and the formation of the non-interconnecting pores. Thus, reducing the membrane permeability by preventing or reducing the water pathways across the membrane. Besides, sintering at a high temperature can cause the elimination of the hydroxyl group from the membrane surface and reduced the hydrophilic property of the ceramic membrane.

The separation mechanism of a membrane is based on the size exclusion. The capability in retaining the small ionic size of water contaminants such as heavy metal ions (Pb^{2+}) using MF and UF type membrane is not possible. The Pb^{2+} ions dissociate in water is having a radius of 0.119 nm. Then, the relative difference between the membrane pore size and Pb^{2+} ions size it can pass through the membrane pore to the permeate side. Hence, advancing the adsorptive properties to the ceramic membrane can give a solution to this issue when using MF or UF type membrane for heavy metal ions removal. Using inorganic particles as an adsorbent for wastewater treatment had prone to the agglomeration of the inorganic particles due to the Van der Waals forces when dispersed in a solution for the adsorption process. Depositing or embedded the inorganic particles on a substrate can overcome the issue of particles agglomeration. For this purpose, the MF and UF membrane range can be used as the substrate for the development of an advance ceramic membrane. This can be done by undergoing modification to the ceramic substrate with an inorganic material. Hence, the deposition of inorganic material with the adsorptive properties allow the membrane to act as an adsorptive membrane. Thus, the small sizes of the monovalent ions which cannot be retained by the MF or UF membrane range through size exclusion mechanism can be adsorbed by the membrane during the filtration process. Therein, provide a single solution to overcome the issues of porous ceramic membrane range to separate small sizes of particulates by separative and inorganic particles agglomeration for adsorption process.

Another issue that arises from the membrane separation process is the membrane fouling phenomenon. There is no exception for the ceramic membrane even though the fouling rate is lower than the polymeric membrane. The ceramic membrane will lose its nature of the hydrophilic properties efficacy over time to resist the membrane fouling. The fouling phenomenon occurs due to the accumulation of foulants on the membrane surface and pores. Thus, increasing the mass transfer and reducing the membrane flux. The previous study had reports oily type wastewater had caused to the great membrane fouling. This type of wastewater also can be separated using MF or UF type membrane as the oil droplets associate in water is within the membrane range. As a solution to the ceramic hollow fiber membrane fouling issue for the oil type wastewater separation, the membrane surface modification with the hydrophilic coating was introduced. The hydrophilic coating by depositing an inorganic material helps in increasing the membrane flux. Owing to the properties of the inorganic material which also response as a photocatalyst can mitigate oil degradation. Thus, creating a self-cleaned membrane process to prevent the formation of foulants layer on the membrane surface. Considering the opaque ceramic hollow fiber membrane, depositing the inorganic material on the outer surface of the ceramic hollow fiber membrane is favored to activate the inorganic material with light irradiation.

From the above problems stated and the solutions proposed, the iron oxide (Fe_2O_3) was chosen as the depositing inorganic material as it can response both as an adsorbent and as a photocatalyst. The deposition can realize the aim of the study to develop a multifunctional ceramic hollow fiber membrane for a different type of water separation. Thus, embedding and depositing the Fe_2O_3 particles within the porous ceramic membrane can provide the adsorptive and photocatalytic properties to the membrane. However, a possibility prone to the detachment of the depositing Fe_2O_3 is concerned to resolve. The polymer coating approached as a protective film or layer can give a solution to secure the deposited Fe_2O_3 . Thus, it is interesting to study the feasibility of the composite polymer-ceramic hollow fiber membrane for the water separation process.

1.3 Objectives

This study aims to develop a multifunctional ceramic hollow fiber membrane for water separation. To highlight the multi-function of the membrane and to solve the problem issued at sub-chapter 1.2, the specific objectives of the study were listed as below:

1. To study the effect of fabrication condition on the $\text{Al}_2\text{O}_3/\text{YSZ}$ hollow fiber morphology as substrate via dry-wet phase inversion and sintering process
2. To evaluate the effect of iron oxide dispersed across the $\text{Al}_2\text{O}_3/\text{YSZ}$ hollow fiber substrate on the structural properties, physical properties and the adsorptive membrane performance
3. To evaluate the effect of iron oxide deposited on the surface of $\text{Al}_2\text{O}_3/\text{YSZ}$ hollow fiber on the structural properties, physical properties and the performance for oil emulsion separation and self-cleaning membrane properties
4. To study the feasibility of polymer coating on the iron oxide supported $\text{Al}_2\text{O}_3/\text{YSZ}$ hollow fiber membrane

1.4 Scope of the Study

To achieve the objectives in this study, the following scope of the study was performed:

Scope objective 1: fabricating the asymmetric $\text{Al}_2\text{O}_3/\text{YSZ}$ hollow fiber substrate via dry-wet phase inversion spinning process and followed by the sintering process.

1. The composition of the ceramic suspension was varied by using two different particle size of the YSZ particles at 0.3 and 0.01 μm .
2. The sintering temperature was also varied at 1350 and 1400 $^\circ\text{C}$.

3. The structural properties of the hollow fibers produced were observed using scanning electron microscopy (SEM), and the distribution between alumina and YSZ particles was observed with the assistance of the energy-dispersive x-ray spectroscopy (EDX).
4. The physical properties of the hollow fiber produced were characterized using mercury intrusion porosimetry (MIP) to measure the pore size distribution of the hollow fibers. The mechanical strength was also measured using the 3P bending strength test. Then, flux properties of the hollow fibers were measured using pure water by using crossflow pressure-driven filtration system.

Scope objective 2: depositing Fe_2O_3 particles within the $\text{Al}_2\text{O}_3/\text{YSZ}$ hollow fiber substrate via an in-situ hydrothermal process

1. The hydrothermal solution was varied by varying the concentration of iron precursor at 0.05 and 0.2 M to determine the Fe_2O_3 deposition within the $\text{Al}_2\text{O}_3/\text{YSZ}$ hollow fiber substrate. During the hydrothermal-deposition process, both ends of the hollow fiber substrate were not closed or capped.
2. The hydrothermal duration was also varied at 24 h and 48 h to evaluate the effect on the deposited Fe_2O_3 particles within the $\text{Al}_2\text{O}_3/\text{YSZ}$ hollow fiber substrate.
3. The structural properties of the Fe_2O_3 deposited within the $\text{Al}_2\text{O}_3/\text{YSZ}$ hollow fiber substrate were examined using field emission scanning electron microscopy (FESEM) and energy-dispersive x-ray spectroscopy (EDX).
4. The physical properties of the Fe_2O_3 deposited were characterized using Fourier-transform infrared spectroscopy (FTIR), using x-ray diffraction (XRD) and N_2 adsorption-desorption. The flux properties of the hollow fibers were measured using pure water by using crossflow pressure-driven filtration system.
5. The Fe_2O_3 supported $\text{Al}_2\text{O}_3/\text{YSZ}$ hollow fiber membrane performance as an adsorptive membrane were evaluated for lead (Pb) removal. The effect of the pH value of Pb (II) solution, time contact, and initial concentration of Pb (II) solution was studied. The concentration of the Pb (II) ions was measured using atomic absorption spectroscopy (AAS).

Scope objective 3: depositing Fe_2O_3 on the surface of the $\text{Al}_2\text{O}_3/\text{YSZ}$ hollow fiber via an in-situ hydrothermal process.

1. The hydrothermal solution was varied by varying the concentration of iron precursor at 0.05, 0.2 and 0.5 M. For this deposition process, both ends of the hollow fiber were capped with polytetrafluoroethylene (PTFE) tape to avoid the penetration of the hydrothermal solution into the hollow fiber substrate through the lumen.
2. The structural properties of the Fe_2O_3 deposited on top of the hollow fiber were examined using field emission scanning electron microscopy (FESEM). The surface properties of the membrane were examined using atomic force microscopy (AFM).
3. The physical properties of the Fe_2O_3 supported on $\text{Al}_2\text{O}_3/\text{YSZ}$ hollow fiber membrane were characterized by the contact angle. The flux properties of the membranes were measured using pure water by using crossflow pressure-driven filtration system.
4. The performance of the Fe_2O_3 supported on $\text{Al}_2\text{O}_3/\text{YSZ}$ hollow fiber membrane was evaluated for oil emulsion separation. The crossflow pressure-driven filtration system was used to carry out the separation of 1000 mg/L oil emulsion solution. The concentration of the oil emulsion was measured using Uv-vis spectroscopy. The particle size distribution of oil droplets was measured using zeta sizer (DLS Malvern).
5. The self-cleaning properties of the Fe_2O_3 supported on $\text{Al}_2\text{O}_3/\text{YSZ}$ hollow fiber membrane were evaluated by a photo-induced filtration process, where the light was illuminated during the filtration process. The oil fluxes and rejections were measured.

Scope objective 4: coating polymer layer on Fe₂O₃ supported Al₂O₃/YSZ hollow fiber membrane

1. Coating the Fe₂O₃ supported on Al₂O₃/YSZ hollow fiber membrane with UV curable resin via dip coating and UV curing process.
2. The structural properties of the UV curable resin coating were observed using field emission scanning electron microscopy (FESEM). The surface properties of the membrane were examined using atomic force microscopy (AFM) and contact angle.
3. The interaction between UV curable resin towards the membrane was analyzed using x-ray diffraction (XRD) and Fourier-transform infrared spectroscopy (FTIR) analysis.
4. The feasibility of the coated membrane with the UV curable resin was evaluated for 1000 mg/L of humic acid removal using sweeping liquid crossflow filtration system. The concentration of the humic acid solution was determined using Uv-vis.

1.5 Significant of Study

This study contributed to the knowledge of the development of multifunctional ceramic hollow fiber membrane for water separation. The different water pollutants in aqueous water can be treated using the same Fe₂O₃ supported Al₂O₃/YSZ hollow fiber membrane. The simultaneous synthesis and deposition of inorganic material via in-situ hydrothermal process within the ceramic hollow fiber substrate are exposed in this study. With the different setup and hydrothermal conditions during the hydrothermal process, the inorganic material can be deposited on top or within across the porous hollow fiber substrate in one-pot. Also, the knowledge on the polymeric coating on the ceramic membrane via UV curing process is defined in this study as the topic regarding this process is not well reported in previously. Then, the feasibility of the membrane for a different type of wastewater treatment is enclosed in this study. First, for the treatment of heavy metal solution, the deposition of inorganic material (adsorbent) within the porous structure of the ceramic membrane had improved the adsorptive

properties of the membrane. Second, as for the oily wastewater treatment, the deposition of inorganic material (photocatalyst) on top of the membrane enables for improving the membrane's flux by improving the hydrophilicity properties of the membrane surface and also enable for the self-cleaning membrane process with the assisted of light irradiation. Third and last, the polymer coating had made the porous ceramic membrane feasible for forward osmosis (FO) application.

The morphology of the ceramic membrane can be categorized into a symmetric and asymmetric structure. The symmetric structure is having the homogeneous pore size distribution across the membrane cross-sectional. Meanwhile, an asymmetrical structure possesses a change in pore size distribution across the membrane cross-sectional. As illustrates in Figure 2.2, the asymmetric membrane consists of a thin as an active layer on the top, an intermediate porous layer and more porous layer as the support at the bottom part. The outer active layer plays a key role in the separation process and the substrate provides the mechanical support to the membrane. Moreover, all layers can be made of the same material or different materials (called a composite ceramic membrane). Where, in a composite ceramic membrane, the properties of the membrane can be tailored depending on the material used in each layer with multi-step of fabrication process [5]. Furthermore, the membrane process can be further classified into microfiltration (MF), ultrafiltration (UF), nanofiltration (NF) and reverse osmosis (RO) according to the pore sizes of the membrane in the pressure-driven membrane processes.

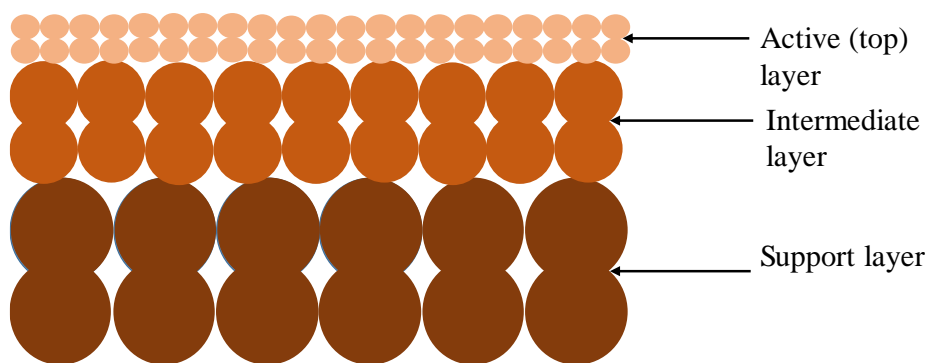


Figure 2.2 The illustration of an asymmetric ceramic membrane.

2.2 Fabrication of an Asymmetric Ceramic Hollow Fiber Membrane

Fabrication of ceramic membrane involves with three main steps: (1) preparation of a homogeneous ceramic suspension containing ceramic powder, solvent, polymer binder and additive; (2) packing and shaping the ceramic suspension into a specific geometry; and (3) consolidation of the ceramic particles by the sintering

REFERENCES

1. Samaei M. S., Gato-trinidad S. and Altaee A. The application of pressure-driven ceramic membrane technology for the treatment of industrial wastewaters – A review. *Separation and Purification Technology*. 2018 (200) 198–220.
2. Paiman. S. H., Rahman M. A., Othman M. H. D., Ismail A. F., Jaafar J. and Aziz A. A. Morphological study of yttria-stabilized zirconia hollow fiber membrane prepared using phase inversion/sintering technique. *Ceramics International*. 2015 (41) 12543–12553.
3. Zhang X., Suo S., Jiang Y., Chang Q., Ji Q. and Liu X. Microstructure evolution and properties of YSZ hollow fiber microfiltration membranes prepared at different suspension solid content for water treatment. *Desalination and Water Treatment*. 2016 (45) 21273–21285.
4. Alresheedi M. T., Barbeau B. and Basu O. D. Comparison of NOM fouling and cleaning of ceramic and polymeric membrane during water treatment. *Separation and Purification Technology*. 2019 (209) 452–460.
5. Abadikhah H., Wang J. W., Xu X. and Agathopoulos S. SiO₂ nanoparticles modified Si₃N₄ hollow fiber membrane for efficient oily wastewater microfiltration. *Journal of Water Process Engineering*. 2019 (29) 100799.
6. Loeb S. and Sourirajan S. Sea Water Demineralization by Means of an Osmotic Membrane. *Advances in Chemistry American Chemical Society*. 1963 (38) 117–132.
- 7.. Droushiotis N., Othman M. H. D., Doraswami U., Wu Z., Kelsall G. and Li K. Novel co-extruded electrolyte-anode hollow fibers for solid oxide fuel cells. *Electrochemistry Communications*. 2009 (11) 1799–1802.
8. Hubadillah S. K., Harun Z., Othman M. H. D., Ismail A. F., and Gani P. Effect of kaolin particle size and loading on the characteristics of kaolin ceramic support prepared via phase inversion technique. *Journal of Asian Ceramic Societies*. 2016 (4) 164–177.

9. Liu S., Li K. and Hughes R. Preparation of porous aluminium oxide (Al_2O_3) hollow fiber membranes by a combined phase-inversion and sintering method. *Ceramics International*. 2003 (29) 875–881.
10. Kingsbury B. F. K. and Li K. A morphological study of ceramic hollow fiber membranes. *Journal of Membrane Science*. 2009 (328) 134–140.
11. Kingsbury B. F. K., Wu Z. and Li K. A morphological study of ceramic hollow fiber membranes: A perspective on multifunctional catalytic membrane reactors. *Catalysis Today*. 2010 (156) 306–315.
12. Liu Y. and Li K. Preparation of $\text{SrCe}_{0.95}\text{Yb}_{0.05}\text{O}_{3-a}$ hollow fiber membranes: Study on sintering processes. *Journal of Membrane Science*. 2005 (259) 47–54.
13. Wei C. C., Chen O. Y., Liu Y., and Li K. Ceramic asymmetric hollow fiber membranes - One step fabrication process. *Journal of Membrane Science* 2008 (320) 191–197.
14. Fung Y. L. E. and Wang H. Nickel aluminate spinel reinforced ceramic hollow fiber membrane. *Journal of Membrane Science*. 2014 (450) 418–424.
15. Wang B., Lee M. and Li K. YSZ-Reinforced Alumina Multi-Channel Capillary Membranes for Micro-Filtration. *Membranes*. 2015 (6) 1–8.
16. Wang S., Tian J., Wang Q., Zhao Z., Cui F. and Li G. Low-temperature sintered high-strength CuO doped ceramic hollow fiber membrane: Preparation, characterization and catalytic activity. *Journal of Membrane Science*. 2019 (570–571) 333–342.
17. Arab A., Sktani Z. D. I., Zhou Q., Ahmad Z. A. and Chen P. Effect of MgO Addition on the Mechanical and Dynamic Properties of Zirconia Toughened alumina (ZTA) Ceramics. *Materials*. 2019 (12) 1 – 14.
18. Zhang X., Lin B., Ling Y., Dong Y., Fang D., Meng G. and Liu X. Highly permeable porous YSZ hollow fiber membrane prepared using ethanol as external coagulant. *Journal of Alloys and Compounds*. 2010 (494) 366–371.
19. Adam M. R., Othman M. H. D., Puteh M. H., Ismail A. F., Mustafa A., Rahman M. A. and Jaafar J. Impact of sintering temperature and pH of feed solution on adsorptive removal of ammonia from wastewater using clinoptilolite based hollow fiber ceramic membrane. *Journal of Water Process Engineering*. 2020 (33) 101063.

20. Jamil S. M., Othman M. H. D., Rahman M. A., Jaafar J., Mohamed M. A., Yusop M. Z. M., Ismail A. F. and Tanemura M. Dual-layer hollow fiber MT-SOFC using lithium doped CGO electrolyte fabricated via phase-inversion technique. *Solid State Ionics*. 2017 (304) 113–125.
21. Jamil S. M., Othman M. H. D., Rahman M. A., Jaafar J., Mohamed M. A., Yusop M. Z. M., Ismail A. F., Honda S. and Iwamoto Y. Properties and performance evaluation of dual-layer ceramic hollow fiber with modified electrolyte for MT-SOFC. *Renewable Energy*. 2019 (134) 1423–1433.
22. Khan I. U., Othman M. H. D., Ismail A. F., Matsuura T., Hashim H., Nordin N. A., H. M., Rahman M. A., Jaafar J. and Jilani A. Status and improvement of dual-layer hollow fiber membranes via co-extrusion process for gas separation: A review. *Journal of Natural Gas Science and Engineering*. 2018 (52) 215–234.
23. Azmi N. F. A. N., Abdullah N., Pauzi M. Z. M., Rahman M. A., Abas K. H., Aziz A. A., Othman M. H. D., Jaafar J. and Ismail A. F. Highly permeable photo-catalytic mesoporous aluminum oxide membrane for oil emulsion separation. *Journal of the Australian Ceramic Society*. 2018 (55) 323 – 335.
24. Zhang H., Taymazov D., Li M. P., Huang Z. H., Liu W. L., Zhang X., Ma X. H. and Xu Z. L. Construction of MoS₂ composite membranes on ceramic hollow fibers for efficient water desalination. *Journal of Membrane Science*. 2019 (592) 117369.
25. Chen X., Qi T., Zhang Y., Wang T., Qiu M., Cui Z. and Fan Y. Facile pore size tuning and characterization of nanoporous ceramic membranes for the purification of polysaccharide. *Journal of Membrane Science*. 2020 (597) 117631.
26. Dhaka S., Kumar R., Deep A., Kurade M. B., Ji S. and Jeon B. H. Metal–organic frameworks (MOFs) for the removal of emerging contaminants from aquatic environments. *Coordination Chemistry Reviewers*. 2019 (380) 330–352.
27. Liu X., Wang C., Wang B. and Li K. Novel Organic-Dehydration Membranes Prepared from Zirconium Metal-Organic Frameworks. *Advanced Functional Materials*. 2017 (27) 1–6.

28. Abdullah N., Rahman M. A., Othman M. H. D., Jaafar J. and Aziz A. A. Preparation, characterizations and performance evaluations of alumina hollow fiber membrane incorporated with UiO-66 particles for humic acid removal. *Journal of Membrane Science*. 2018 (563) 162–174.
29. Lau W. J., Ismail A. F., Misdan N. and Kassim M. A. A recent progress in thin film composite membrane: A review. *Desalination*. 2012 (287) 190–199.
30. Xia L., Ren J., Weyd M. and McCutcheon J. R. Ceramic-supported thin film composite membrane for organic solvent nanofiltration. *Journal of Membrane Science*. 2018 (563) 857–863.
31. Chong J. Y. and Wang R. From micro to nano: Polyamide thin film on microfiltration ceramic tubular membranes for nanofiltration. *Journal of Membrane Science*. 2019 (587) 117161.
32. Dong Z., Zhu H., Hang Y., Liu G. and Jin W. Polydimethylsiloxane (PDMS) Composite Membrane Fabricated on the Inner Surface of a Ceramic Hollow Fiber: From Single-Channel to Multi-Channel. *Engineering*. 2020 (6) 89–99.
33. Hubadillah S. K., Tai Z. S., Othman M. H. D., Harun Z., Jamalludin M. R., Rahman M. A., Jaafar J. and Ismail A. F. Hydrophobic ceramic membrane for membrane distillation: A mini review on preparation, characterization, and applications. *Separation and Purification Technology*. 2019 (217) 71–84.
34. Chen X., Gao X., Fu K., Qiu M., Xiong F., Ding D., Cui Z., Wang Z., Fan Y. and Drioli E. Tubular hydrophobic ceramic membrane with asymmetric structure for water desalination via vacuum membrane distillation process. *Desalination*. 2018 (443) 212–220.
35. Cui Y., Chen Z. and Liu X. Progress in Organic Coatings Preparation of UV-curing polymer-ZrO₂ hybrid nanocomposites via auto-hydrolysis sol-gel process using zirconium oxychloride octahydrate coordinated with organic amine. *Progress in Organic Coatings*. 2016 (100) 178–187.
36. Sangermano M., Malucelli G., Priola A., and Manea M. Synthesis and characterization of acrylate–oxetane interpenetrating polymer networks through a thermal-UV dual cure process. *Progress in Organic Coatings*. 2006 (55) 225–230.

37. Closser R.G, Lillethorup M., Bergsman D. S and Bent S. F. Growth of a Surface-Tethered, All-Carbon Backboned Fluoropolymer by Photoactivated Molecular Layer Deposition. *Applied Materials & Interfaces*. 2019 (11) 21988–21997.
38. Lu J. P., Chen L. and Song R. G. Effects of SiO₂ particle size on the corrosion resistance of fluoropolymer/ SiO₂ composite coatings. *Surface Engineering*. 2019 (35) 440–449.
39. Boschet. F. and Ameduri B. (Co) polymers of Chlorotrifluoroethylene: Synthesis, Properties, and Applications. *Chemical Reviews*. 2013 (114) 927–980.
40. Honda K., Morita M., Otsuka H. and Takahara A. Molecular Aggregation Structure and Surface Properties of Poly(fluoroalkyl acrylate) Thin Films. *Macromolecules*. 2005 (38) 5699–5705.
41. Zhang H., Song J. and Liu C. Immobilization of α -Fe₂O₃ Nanoparticles on PET Fiber by Low Temperature Hydrothermal Method. *Industrial & Engineering Chemistry Research*. 2013 (52) 7403–7412.
42. Ahmad S. H., Jamil S. M., Othman M. H. D., Rahman M. A., Jaafar J., and Ismail A. F. Co-extruded dual-layer hollow fiber with different electrolyte structure for a high temperature micro-tubular solid oxide fuel cell. *International Journal of Hydrogen Energy* 2017 (42) 9116–9124.
43. Kim J. and Bruggen B. V. D. The use of nanoparticles in polymeric and ceramic membrane structures: Review of manufacturing procedures and performance improvement for water treatment. *Environmental Pollution*. 2010 (158) 2335–2349.
44. Chang Q., Zhou J. E., Wang Y., Wang J. and Meng G. Hydrophilic modification of Al₂O₃ microfiltration membrane with nano-sized γ -Al₂O₃ coating. *Desalination*. 2010 (262) 110–114.
45. Zhou J. E., Chang Q., Wang Y., Wang J. and Meng G. Separation of stable oil-water emulsion by the hydrophilic nano-sized ZrO₂ modified Al₂O₃ microfiltration membrane. *Separation and Purification Technology*. 2010 (75) 243–248.

46. Pauzi M. Z. M., Mahpoz M. N., Abdullah N., Rahman M. A., Abas K. H., Aziz A. A., Padzillah M. H., Othman M. H. D., Jaafar J. and Ismail A. F. Feasibility study of CAU-1 deposited on alumina hollow fiber for desalination applications. *Separation and Purification Technology*. 2019 (217) 247–257.
47. Zaspalis V., Pagana A. and Sklari S. Arsenic removal from contaminated water by iron oxide sorbents and porous ceramic membranes. *Desalination*. 2007 (217) 167–180.
48. Pagana A. E., Sklari S. D., Kikkinides E. S. and Zaspalis V. T. Microporous ceramic membrane technology for the removal of arsenic and chromium ions from contaminated water. *Microporous Mesoporous Materials*. 2008 (110) 150–156.
49. Yin N., Wang K., Wang L. and Li Z. Amino-functionalized MOFs combining ceramic membrane ultrafiltration for Pb (II) removal. *Chemical Engineering Journal*. 2016 (306) 619–628.
50. Adam M. R., Salleh N. M., Othman M. H. d., Matsuura T., Ali M. H., Puteh M. H., Ismail A. F., Rahman M. A. and Jaafar J. The adsorptive removal of chromium (VI) in aqueous solution by novel natural zeolite based hollow fiber ceramic membrane. *Journal of Environmental Management*. 2018 (224) 252–262.
51. Muhamad N., Abdullah N., Rahman M. A., Abas K. H., Aziz A. A., Othman M. H. D., Jaafar J. and Ismail A. F. Removal of nickel from aqueous solution using supported zeolite-Y hollow fiber membranes. *Environmental Science and Pollution Research*. 2018 (25) 19054–19064.
52. Choudhury P., Mondal P., Majumdar S., Saha S. and Sahoo G. C. Preparation of ceramic ultrafiltration membrane using green synthesized CuO nanoparticles for chromium (VI) removal and optimization by response surface methodology. *Journal of Cleaner Production*. 2018 (203) 511–520.
53. Rajan S., Firdaus N. N. M., Appukutty M. and Ramasamy K.. Effects of climate changes on dissolved heavy metal concentrations among recreational park tributaries in Pahang, Malaysia. *Biomedical Research*. 2012 (23) 23–30.
54. Chowdhury S., Mazumder M. A. J., Al-attas O. and Husain T. Heavy metals in drinking water: Occurrences, implications, and future needs in developing countries. *Science of the Total Environment*. 2016 (569–570) 476–488.

55. Barakat M. A. New trends in removing heavy metals from industrial wastewater. *Arabian Journal of Chemistry*. 2011 (4) 361–377.
56. Jaishankar M., Tseten T., Anbalagan N., Mathew B. B. and Beeregowda K. N. Toxicity, mechanism and health effects of some heavy metals. *Interdisciplinary Toxicology*. 2014 (7) 60–72.
57. Murcia M., Ballester F., Enning A. M., Iniguez C., Valvi D., Basterrechea M., Rebagliato M., Vioque J., Maruri M., Tardon A., Galan I. R., Vrijheid M. and Llop S. Prenatal mercury exposure and birth outcomes. *Environmental Research*. 2016 (151) 11–20.
58. Kokkinos E., Simeonidis K., Pinakidou F., Katsikini M. and Mitrakas M. Optimization of tetravalent manganese ferrihydrite's negative charge density: A high-performing mercury adsorbent from drinking water. *Science of the Total Environment*. 2017 (574) 482–489.
59. Huang S. H. and Chen D. H. Rapid removal of heavy metal cations and anions from aqueous solutions by an amino-functionalized magnetic nano-adsorbent. *Journal of Hazardous Materials*. 2009 (163) 174–179.
60. Lee A. Y. W., Lim S. F., Chua S. N. D., Sanauallah K., Bains R. and Abdullah M. O. Adsorption Equilibrium for Heavy Metal Divalent Ions (Cu^{2+} , Zn^{2+} , and Cd^{2+}) into Zirconium-Based Ferromagnetic Sorbent. *Advances in Materials Science and Engineering*. 2017 (2017) 1–13.
61. Lin S., Liu L., Yang Y., and Lin K. Study on preferential adsorption of cationic-style heavy metals using amine-functionalized magnetic iron oxide nanoparticles (MIONPs-NH₂) as efficient adsorbents. *Applied Surface Science*. 2017 (407) 29–35.
62. Roychoudhury P., Majumdar S., Sarkar S. and Kundu B. Performance investigation of Pb (II) removal by synthesized hydroxyapatite based ceramic ultrafiltration membrane: Bench scale study. *Chemical Engineering Journal*. 2019 (355) 510–519.
63. Farghali A. A., Bahgat M., Allah A. E. and Khedr M. H. Adsorption of Pb (II) ions from aqueous solutions using copper oxide nanostructures. *Beni-Suef University Journal Basic and Applied Sciences*. 2013 (2) 61–71.

64. Shahzad H. K., Hussein M. A., Patel F., Al-Aqeeli N., Atieh M. A. and Laoui T.. Synthesis and characterization of alumina-CNT membrane for cadmium removal from aqueous solution. *Ceramics International*. 2018 (44) 17189–17198.
65. Zhang S., Cheng F., Tao Z., Gao F. and Chen J. Removal of nickel ions from wastewater by Mg(OH)₂/MgO nanostructures embedded in Al₂O₃ membranes. *Journal of Alloys Compounds*. 2006 (426) 281–285.
66. Chougui A., Zaiter K., Belouatek A. and Asli B. Heavy metals and color retention by a synthesized inorganic membrane. *Arabian Journal of Chemistry*. 2014 (7) 817–822.
67. Choudhury P. R., Majumdar S., Sahoo G. C., Saha S. and Mondal P. High pressure ultrafiltration CuO/hydroxyethyl cellulose composite ceramic membrane for separation of Cr (VI) and Pb (II) from contaminated water. *Chemical Engineering Journal*. 2017 (336) 570–578.
68. Liu W., Wang D., Soomro R. A., Fu F., Qiao N., Yu Y., Wang R and Xu B. Ceramic supported attapulgite-graphene oxide composite membrane for efficient removal of heavy metal contamination. *Journal Membrane Science*. 2019 (591) 117323.
69. Molinari R., Lavorato C., and Argurio P. Recent progress of photocatalytic membrane reactors in water treatment and in synthesis of organic compounds. A review. *Catalysis Today*. 2017 (281) 144–164.
70. Fujishima A., Zhang X. and Tryk D. TiO₂ photocatalysis and related surface phenomena. *Surface Science Reports*. 2008 (63) 515–582.
71. Wang Z. and Mi B. Environmental Applications of 2D Molybdenum Disulfide (MoS₂) Nanosheets. *Environmental Science & Technology*. 2017 (51) 8229–8244.
72. Domingo E., Beltrán A., Sanchis R., García T., Solsona B. and Galindo F. Photocatalytic Activity of Mesoporous α -Fe₂O₃ Synthesized via Soft Chemistry and Hard Template Methods for Degradation of Azo Dye Orange II. *Catalysis Letters*. 2018 (148) 1289–1295.
73. Xu P., Zeng G. M., Huang D. L., Feng C. L., Hu S., Zhao M. H., Lai C., Wei Z., Huang C., Xie G. X and Liu Z. F. Use of iron oxide nanomaterials in wastewater treatment: A review. *Science of the Total Environment*. 2012 (424) 1–10.

74. Henderson M. A. A surface science perspective on TiO₂ photocatalysis. *Surface Science Reports*. 2011 (66) 185–297.
75. Zhang X., Wang D. K., Lopez D. R. S. and Costa J. C. D. Fabrication of nanostructured TiO₂ hollow fiber photocatalytic membrane and application for wastewater treatment. *Chemical Engineering Journal*. 2014 (236) 314–322.
76. Du L., Liu W., Hu S., Wang Y. and Yang J. Preparation and photocatalytic properties of macroporous honeycomb alumina ceramics used for water purification. *Journal of European Ceramic Society*. 2014 (34) 731–738.
77. Abdullah N., Rahman M. A., Othman M. H. D., Ismail A. F., Jaafar J. and Aziz A. A. Preparation and characterization of self-cleaning alumina hollow fiber membrane using the phase inversion and sintering technique. *Ceramics International*. 2016 (42) 12312–12322.
78. Wang S., Tian J., Wang Q., Xiao F., Gao S. and Shi W. Development of CuO coated ceramic hollow fiber membrane for peroxymonosulfate activation: a highly efficient singlet oxygen-dominated oxidation process for bisphenol a degradation. *Applied Catalysis B: Environmental*. 2019 (256) 117783.
79. Mohtor N. H., Othman M. H. D., Bakar S. A., Kurniawan T. A., Dzinun H., Norrdin M. N. A. M., and Rajis Z. Synthesis of Nanostructured Titanium Dioxide Layer onto Kaolin Hollow Fiber Membrane via Hydrothermal Method for Decolourisation of Reactive Black 5. *Chemosphere*. 2018 (208) 595–605.
80. Wandera D., Wickramasinghe S. R. and Husson S. M. Modification and characterization of ultrafiltration membranes for treatment of produced water. *Journal of Membrane Science*. 2011 (373) 178–188.
81. Bengani-Lutz P., Zaf R. D., Culfaz-Emecen P. Z. and Asatekin A. Extremely fouling resistant zwitterionic copolymer membranes with ~ 1 nm pore size for treating municipal, oily and textile wastewater streams. *Journal of Membrane Science* 2017 (543) 184–194.
82. Cheryan M. and Rajagopalan N. Membrane processing of oily streams. Wastewater treatment and waste reduction. *Journal of Membrane Science*. 1998 (151) 13–28.
83. Yu L., Han M. and He F. A review of treating oily wastewater. *Arabian Journal of Chemistry*. 2017 (10) 1913–1922.

84. Laffon B., Pásaro E. and Valdiglesias V. Effects of exposure to oil spills on human health: Updated review. *Journal of Toxicology and Environmental Health, Part B*. 2016 (19) 105–128.
85. Zhang X., Hu J., Chang Q., Wang Y., Zhou J., Zhou T., Jiang Y. and Liu X. Influences of internal coagulant composition on microstructure and properties of porous YSZ hollow fiber membranes for water treatment. *Separation and Purification Technology*. 2015 (147) 337–345.
86. Huang S., Ras R. H. A. and Tian X. Antifouling membranes for oily wastewater treatment: Interplay between wetting and membrane fouling. *Colloid Interface Science*. 2018 (36) 90–109.
87. Carpintero-Tepole V., Fuente E. B, and Torrestiana-Sánchez B. Microfiltration of oil in water (O/W) emulsions: Effect of membrane microstructure and surface properties. *Chemical Engineering Research and Design*. 2017 (126) 286–296.
88. Zhang W., Luo J., Ding L. and Jaffrin M. Y. A review on flux decline control strategies in pressure-driven membrane processes. *Industrial Engineering Chemistry Research*. 2015 (54) 2843–2861.
89. Chang Q., Zhang L., Liu X., Peng D. and Meng G. Preparation of crack-free ZrO₂ membrane on Al₂O₃ support with ZrO₂-Al₂O₃ composite intermediate layers. *Journal of Membrane Science*. 2005 (250) 105–111.
90. Matin A., Baig U., Gondal M. A., Akhtar S. and Zubair S. M. Facile fabrication of superhydrophobic/superoleophilic microporous membranes by spray-coating ytterbium oxide particles for efficient oil-water separation. *Journal of Membrane Science*. 2018 (548) 390–397.
91. Jeong Y., Kim Y., Jin Y., Hong S. and Park C. Comparison of filtration and treatment performance between polymeric and ceramic membranes in anaerobic membrane bioreactor treatment of domestic wastewater. *Separation and Purification Technology*. 2018 (199) 182–188.
92. Chang Q., Zhou J., Wang Y., Liang J., Zhang X., Cerneaux S., Wang X., Zhu Z. and Dong Y. Application of ceramic microfiltration membrane modified by nano-TiO₂ coating in separation of a stable oil-in-water emulsion. *Journal of Membrane Science*. 2014 (456) 128–133.

93. Lu D., Cheng W., Zhang T., Lu X., Liu Q., Jiang J. and Ma J. Hydrophilic Fe_2O_3 dynamic membrane mitigating fouling of support ceramic membrane in ultrafiltration of oil/water emulsion. *Separation and Purification Technology*. 2016 (165) 1–9.
94. Sun S., Yao H., Fu W., Hua L. and Zhang G. Reactive Photo-Fenton ceramic membranes: Synthesis , characterization and antifouling performance. *Water Research*. 2018 (144) 690–698.
95. Fard A. K., Rhadfi T., Mckay G., Al-marri M., Abdala A., Hilal N. and Hussien M. A. Enhancing oil removal from water using ferric oxide nanoparticles doped carbon nanotubes adsorbents. *Chemical Engineering Journal*. 2016 (293) 90–101.
96. Zhou Y., Tang X., Xu Y. and Lu J. Effect of quaternary ammonium surfactant modification on oil removal capability of polystyrene resin. *Separation and Purification Technology*. 2010 (75) 266–272.
97. Zhou J. E., Chang Q., Wang Y., Wang J. and Meng G. Separation of stable oil-water emulsion by the hydrophilic nano-sized ZrO_2 modified Al_2O_3 microfiltration membrane. *Separation and Purification Technology*. 2010 (75) 243–248.
98. Zhu L., Chen M., Dong Y., Tang C. Y., Huang A. and Li L. A low-cost mullite-titania composite ceramic hollow fiber microfiltration membrane for highly efficient separation of oil-in-water emulsion. *Water Research*. 2016 (90) 277–285.
99. Suresh K. and Pugazhenti G. Cross flow microfiltration of oil-water emulsions using clay based ceramic membrane support and TiO_2 composite membrane. *Egyptian Journal of Petroleum*. 2017 (26) 679–694.
100. Alias N. H., Jaafar J., Samitsu S., Matsuura T., Ismail A. F., Othman M. H. D., Rahman M. A., Othman N. H., Abdullah N., Paiman S. H., Yusof N. and Aziz F. Photocatalytic nanofiber-coated alumina hollow fiber membranes for highly efficient oilfield produced water treatment. *Chemical Engineering Journal*. 2019 (360) 1437–1446.
101. Wang M., Liao L., Zhang X., and Li Z. Adsorption of low concentration humic acid from water by palygorskite. *Applied Clay Science*. 2012 (67) 164–168.

102. Wang T., Li Y., Qu G., Sun Q. and Liang D. Enhanced removal of humic acid from micro-polluted source water in a surface discharge plasma system coupled with activated carbon. *Environment Science Pollution Research*. 2017 (24) 21591–21600.
103. Wang T., Qu G., Ren J., Yan Q. and Sun Q. Evaluation of the potentials of humic acid removal in water by gas phase surface discharge plasma. *Water Research*. 2016 (89) 28–38.
104. Zhou X. F., Liang J. P., Zhao Z. L., Yuan H., Qiao J. J., Xu Q. N., Wang H. L., Wang W. C., and Yang D. Z.. Ultra-high synergetic intensity for humic acid removal by coupling bubble discharge with activated carbon. *Journal of Hazardous Materials*. 2021 (403) 123626.
105. Dehgani M. H., Zarei A., Mesdaghinia A., Nabizadeh R., Alimohammadi M., Afsharnia M. and McKay G. Production and application of a treated bentonite–chitosan composite for the efficient removal of humic acid from aqueous solution. *Chemical Engineering Research and Design*. 2018 (140) 102–115.
106. Khan S., Kim J., Sotto A. and Van Der Bruggen B., Humic acid fouling in a submerged photocatalytic membrane reactor with binary TiO₂–ZrO₂ particles. *Journal of Industrial and Engineering Chemistry* 2015 (21) 779–786.
107. Imyim A. and Prapalimrungsi E. Humic acids removal from water by aminopropyl functionalized rice husk ash. *Journal of Hazardous Materials*. 2010 (184) 775–781.
108. Woo K., Hong J., Choi S., Lee H. W., Ahn J. P., Kim C. S. and Lee S. W. Easy Synthesis and Magnetic Properties of Iron Oxide Nanoparticles. *Chemistry of Materilas*. 2004 (16) 2814–2818.
109. Hosseini S. G., Ahmadi R., Ghavi A. and Kashi A. Synthesis and characterization of α -Fe₂O₃ mesoporous using SBA-15 silica as template and investigation of its catalytic activity for thermal decomposition of ammonium perchlorate particles. *Powder Technology*. 2015 (278) 316–322.
110. Solsona B., Garcia T., Sanchis R., Soriano M. D., Moreno M., Rodriguez-Castellon E., Aguoram S., Dejoz A. and Nieto L. M. L. Total oxidation of VOCs on mesoporous iron oxide catalysts : Soft chemistry route versus hard template method. *Chemical Engineering Journal*. 2016 (290) 273–281.

111. Liang H., Liu K. and Ni Y. Synthesis of mesoporous α -Fe₂O₃ via sol–gel methods using cellulose nano-crystals (CNC) as template and its photocatalytic properties. *Materials Letters*. 2015 (159) 218–220.
112. Ilankoon N. Use of iron oxide magnetic nanosorbents for Cr (VI) removal from aqueous solutions: A review. *Journal of Engineering Research and Applications*. 2014 (10) 55–63.
113. Kumari M., Pittman C. U. and Mohan D. Heavy metals [Chromium (VI) and lead (II)] removal from water using mesoporous magnetite (Fe₃O₄) nanospheres. *Journal of Colloid Interface Science*. 2014 (442) 120–132.
114. Olivera S., Hu C., Nagananda G. S., Reddy N., Venkatesh K., Muralidhara H. B., Inamuddin and Asiri A. M. The adsorptive removal of Cr(VI) ions and antibacterial activity studies on hydrothermally synthesized iron oxide and zinc oxide nanocomposite. *Journal of Taiwan Institute of Chemical Engineers*. 2018 (93) 342–349.
115. Uggas L., Romeo V., Tedeschi E., Brunetti A. and Quarantelli M. Superparamagnetic iron oxide nanocolloids in MRI studies of neuroinflammation. *Journal of Neuroscience Methods*. 2018 (310) 12–23.
116. Saritas S., Kundakci M., Coban O., Tuzemen S. and Yildirim M. Ni:Fe₂O₃, Mg: Fe₂O₃ and Fe₂O₃ thin films gas sensor application. *Physica B: Condensed Matter*. 2018 (541) 14–18.
117. Nizamuddin S. Siddiqui M. T. H., Mubarak N. M., Baloch H. A., Abdullah E. C., Mazari S. A., Griffin G. J., Srinivasan M. P. and Tanksale A. Iron Oxide Nanomaterials for the Removal of Heavy Metals and Dyes From Wastewater. Elsevier Inc., Chapter 17 2019 447–472.
118. Vardhan K. H., Kumar P. S. and Panda R. C. A review on heavy metal pollution, toxicity and remedial measures: Current trends and future perspectives. *Journal of Molecular Liquids*. 2019 (290) 111197.
119. Wu D., Wang Y., Li Y., Wei Q., Hu L., Yan T., Feng R., Yan L. and Du B. Phosphorylated chitosan/CoFe₂O₄ composite for the efficient removal of Pb (II) and Cd (II) from aqueous solution: Adsorption performance and mechanism studies. *Journal of Molecular Liquids*. 2019 (277) 181–188.
120. Fu F. and Wang Q. Removal of heavy metal ions from wastewaters: A review. *Journal of Environmental Management*. 2011 (92) 407–418.

121. Liu E. T., Zhao H., Li H., Li G., Liu Y. and Chen R. Hydrothermal synthesis of porous α -Fe₂O₃ nanostructures for highly efficient Cr(VI) removal. *New Journal of Chemistry*. 2014 (38) 2911–2916.
122. Liu Z., Yu R., Dong Y., Li W. and Zhou W. Preparation of α -Fe₂O₃ hollow spheres, nanotubes, nanoplates and nanorings as highly efficient Cr(VI) adsorbents. *RSC Advances*. 2016 (6) 82854–82861.
123. Wang D., Yang P. and Huang B. Three-dimensional flowerlike iron oxide nanostructures: Morphology, composition and metal ion removal capability. *Materials Research Bulletin*. 2016 (73) 56–64.
124. Cao C. Y., Qu J., Yan W. S., Zhu J. F., Wu Z. Y. and Song W. G. Low-Cost Synthesis of Flowerlike α -Fe₂O₃ Nanostructures for Heavy Metal Ion Removal: Adsorption Property and Mechanism. *Langmuir*. 2012 (28) 4573–4579.
125. Lee S. C., Jeong Y., Kim Y. J., Kim H., Lee H. U., Lee Y. C., Lee S. M., Kim H. J., An H. R., Ha M. G., Lee G. W., Lee Y. S. and Lee G. Hierarchically three-dimensional (3D) nanotubular sea urchin-shaped iron oxide and its application in heavy metal removal and solar-induced photocatalytic degradation. *Journal of Hazardous Materials*. 2018 (354) 283–292.
126. Zhang C., Yu Z., Zeng G., Huang B., Dong H., Huang J. Yang Z., Wei J, Hu L. and Zhang Q. Phase transformation of crystalline iron oxides and their adsorption abilities for Pb and Cd. *Chemical Engineering Journal*. 2016 (284) 247–259.
127. Tan Y., Chen M. and Hao Y. High efficient removal of Pb (II) by amino-functionalized Fe₃O₄ magnetic. *Chemical Engineering Journal*. 2012 (191) 104–111.
128. Zhao J., Liu J., Wang W., Nan J., Zhao Z. and Cui F. Highly efficient removal of bivalent heavy metals from aqueous systems by magnetic porous Fe₃O₄-MnO₂: Adsorption behavior and process study. *Chemical Engineering Journal*. 2016 (304) 737–746.
129. Cui X., Liu T., Zhang Z., Wang L., Zuo S. and Zhu W. Hematite nanorods with tunable porous structure: Facile hydrothermal-calcination route synthesis, optical and photocatalytic properties. *Powder Technology*. 2014 (266) 113–119.

130. Mishra M. and Chun D. M. α -Fe₂O₃ as a photocatalytic material: A review. *Applied Catalysis A: General*. 2015 (498) 126–141.
131. Zhang X., Niu Y., Li Y., Hou X., Wang Y., Bai R. and Zhao J. Synthesis, optical and magnetic properties of α -Fe₂O₃ nanoparticles with various shapes. *Materials Letters*. 2013 (99) 111–114.
132. Xu Y., Zhang G., Du G., Sun Y. and Gao D. α -Fe₂O₃ nanostructures with different morphologies: Additive-free synthesis, magnetic properties and visible light photocatalytic properties. *Materials Letters*. 2013 (92) 321–324.
133. Zhou X., Yang H., Wang C., Mao X., Wang Y., Yang Y. and Liu G. Visible Light Induced Photocatalytic Degradation of Rhodamine B on One-Dimensional Iron Oxide Particles. *Journal of Physical Chemistry C*. 2010 (114) 17051–17061.
134. Lassoued A., Lassoued M. S., Dkhil B., Ammar S. and Gadri A. Photocatalytic degradation of methylene blue dye by iron oxide (α -Fe₂O₃) nanoparticles under visible irradiation. *Journal of Materials Science Materials in Electronics*. 2018 (29) 8142–8152.
135. Jiang T., Poyraz A. S., Iyer A., Zhang Y., Luo Z., Zhong W., Miao R., El-Sawy A. M., Guild C. J., Sun Y., Kriz D. A. and Suib S. L. Synthesis of Mesoporous Iron Oxides by an Inverse Micelle Method and Their Application in the Degradation of Orange II under Visible Light at Neutral pH. *Journal of Physical Chemistry C*. 2015 (119) 10454–10468.
136. Lachheb H., Ajala F., Hamrouni A., Houas A., Parrino F. and Palmisano L. Electron transfer in ZnO-Fe₂O₃ in aqueous slurry systems and its effects on visible light photocatalytic activity. *Catalysis Science & Technology*. 2017 (7) 4041–4047.
137. Priyanka and Srivastava V. C. Photocatalytic Oxidation of Dye Bearing Wastewater by Iron Doped Zinc Oxide. *Industrial & Engineering Chemistry Research*. 2013 (52) 17790–17799.
138. Zhu D., Liu S., Chen M., Zhang J. and Wang X. Flower-like-flake Fe₃O₄/g-C₃N₄ nanocomposite: Facile synthesis, characterization, and enhanced photocatalytic performance. *Colloids Surfaces A*. 2018 (537) 372–382.

139. Demirci S., Yurddaskal M., Dikici T. and Sarıoğlu C. Fabrication and characterization of novel iodine doped hollow and mesoporous hematite (Fe_2O_3) particles derived from sol-gel method and their photocatalytic performances. *Journal of Hazardous Materials*. 2018 (345) 27–37.
140. Mukherjee D., Ghosh S., Majumdar S. and Annapurna K. Green synthesis of $\alpha\text{-Fe}_2\text{O}_3$ nanoparticles for arsenic(V) remediation with a novel aspect for sludge management. *Journal of Environmental Chemical Engineering*. 2016 (4) 639–650.
141. Cui H. J., Cai J. K., Zhao H., Yuan B. L., Ai C. L. and Fu M. L. One step solvothermal synthesis of functional hybrid $\gamma\text{-Fe}_2\text{O}_3$ /carbon hollow spheres with superior capacities for heavy metal removal. *Journal of Colloid and Interface Science*. 2014 (425) 131–135.
142. Chakrabarty S. and Chatterjee K. Oriented growth of $\alpha\text{-Fe}_2\text{O}_3$ nanocrystals with different morphology and their optical behavior. *Journal of Crystal Growth*. 2013 (381) 107–113.
143. Tai G., Zhou J., and Guo W. Inorganic salt-induced phase control and optical characterization of cadmium sulfide nanoparticles. *Nanotechnology*. 2010 (21) 175601.
144. Jiao H. and Wang J. Single crystal ellipsoidal and spherical particles of $\alpha\text{-Fe}_2\text{O}_3$: Hydrothermal synthesis, formation mechanism, and magnetic properties. *Journal of Alloys Compounds*. 2013 (577) 402–408.
145. Sreeja V. and Joy P. A. Microwave-hydrothermal synthesis of $\gamma\text{-Fe}_2\text{O}_3$ nanoparticles and their magnetic properties. *Materials Research Bulletin*. 2007 (42) 1570–1576.
146. Li C., Wei Y., Liivat A., Zhu Y. and Zhu J. Microwave-solvothermal synthesis of Fe_3O_4 magnetic nanoparticles. *Materials Letters* 2013 (107) 23–26.
147. Khalil M., Yu J., Liu N. and Lee R. L. Hydrothermal synthesis, characterization, and growth mechanism of hematite nanoparticles. *Journal of Nanoparticle Research*. 2014 (16) 2362.
148. Liang H., Liu K. and Ni Y. Synthesis of mesoporous $\alpha\text{-Fe}_2\text{O}_3$ via sol-gel methods using cellulose nano-crystals (CNC) as template and its photocatalytic properties. *Materials Letters*. 2015 (159) 218–220.

149. Cuong N. D., Hoa N. D., Huo T. T., Khieu D. Q., Quang D. T., Quang V. V. and Hieu N. V. Nanoporous hematite nanoparticles: Synthesis and applications for benzylation of benzene and aromatic compounds. *Journal of Alloys and Compounds*. 2014 (582) 83–87.
150. Zhou J., Zhang Z., Cheng B. and Yu J. Glycine-assisted hydrothermal synthesis and adsorption properties of crosslinked porous α -Fe₂O₃ nanomaterials for p-nitrophenol. *Chemical Engineering Journal*. 2012 (211–212) 153–160.
151. Liang H., Liu K. and Ni Y. Synthesis of mesoporous α -Fe₂O₃ using cellulose nanocrystals as template and its use for the removal of phosphate from wastewater. *Journal of the Taiwan Institute of Chemical Engineers*. 2017 (71) 474–479.
152. Xia Y., Dai H., Jiang H., Zhang L., Deng J. and Liu Y. Three-dimensionally ordered and wormhole-like mesoporous iron oxide catalysts highly active for the oxidation of acetone and methanol. *Journal of Hazardous Materials*. 2011 (186) 84–91.
153. Xie Y., Kocaefe D., Chen C. and Kocaefe Y. Review of Research on Template Methods in Preparation of Nanomaterials. *Journal of Nanomaterials*. 2016 (2016) 1–10.
154. Wang F., Qin X. F., Meng Y. F., Guo Z. L., Yang L. X. and Ming Y. F. Hydrothermal synthesis and characterization of α -Fe₂O₃ nanoparticles. *Materials Science in Semiconductor Processing*. 2013 (16) 802–806.
155. Burukhin A. A., Churagulov B. R., Oleynikov N. N. and Knot'ko A. V. Hydrothermal synthesis of mesoporous iron oxide powders. *New Journal of Chemistry*. 2013 (37) 6–9.
156. An Z., Zhang J., Pan S., and Song G. Novel peanut-like α -Fe₂O₃ superstructures: Oriented aggregation and Ostwald ripening in a one-pot solvothermal process. *Powder Technology*. 2012 (217) 274–280.
157. Lian S., Li H., He X., Kang Z., Liu Y. and Tong S. Hematite homogeneous core/shell hierarchical spheres: Surfactant-free solvothermal preparation and their improved catalytic property of selective oxidation. *Journal of Solid State Chemistry*. 2012 (185) 117–123.
158. Sun P., Wang W., Liu Y., Sun Y., Ma J. and Lu G. Hydrothermal synthesis of 3D urchin-like α -Fe₂O₃ nanostructure for gas sensor. *Sensors Actuators B: Chemical*. 2012 (173) 52–57.

159. Liang J., Li L. and Kang H. Solvothermal synthesis, growth mechanism, and magnetic property of self-assembled 3D multileaf α -Fe₂O₃ superstructures. *Powder Technology*. 2013 (235) 475–478.
160. Zhong L. S., Hu J. S., Liang H. P., Cao A. M., Song W. G. and Wan L. J. Self-assembled 3D flowerlike iron oxide nanostructures and their application in water treatment. *Advanced Materials*. 2006 (18) 2426–2431.
161. K. Li, *Ceramic Membranes for Separation and Reaction*. England: John Wiley and Sons, Ltd. 2007
162. Paiman S. H., Rahman M. A., Uchikoshi T. Nordin N. A. H M., Alias N. H., Abdullah N., Abas K. H., Othman M. H. D., Jaafar J. and Ismail A. F. In situ growth of α -Fe₂O₃ on Al₂O₃/YSZ hollow fiber membrane for oily wastewater. *Separation and Purification Technology*. 2020 (236) .
163. Adam M. R., Salleh N. M., Othman M. H. d., Matsuura T., Ali M. H., Puteh M. H., Ismail A. F., Rahman M. A. and Jaafar J. The adsorptive removal of chromium (VI) in aqueous solution by novel natural zeolite based hollow fiber ceramic membrane. *Journal of Environmental Management*. 2018 (224) 252–262.
164. Fan Z., Zhao Y., Lu M. and Huang H. Ytria stabilized zirconia (YSZ) thin wall structures fabricated using laser engineered net shaping (LENS). *The International Journal of Advanced Manufacturing Technology*. 2019 (105) 4491–4498.
165. Adam M. R., Othman M. H. D., Kadir S. H. S. A., Sokri M. N. M., Tai Z. S., Iwamoto Y., Tanemura M., Honda S., Puteh M. H., Rahman M. A and Jaafar J. Influence of the natural zeolite particle size toward the ammonia adsorption activity in ceramic hollow fiber membrane. *Membranes*. 2020 (10) 1–18.
166. Zhang J., Li L., Li Y. and Yang C. Microwave-assisted synthesis of hierarchical mesoporous nano-TiO₂/cellulose composites for rapid adsorption of Pb²⁺. *Chemical Engineering Journal*. 2017 (313) 1132–1141.
167. Liu Y., Peng M., Jiang H., Xing W., Wang Y. and Chen R. Fabrication of ceramic membrane supported palladium catalyst and its catalytic performance in liquid-phase hydrogenation reaction. *Chemical Engineering Journal*. 2017 (313) 1556–1566.

168. Abdullah N., Gohari R. J., Yusof N., Ismail A. F., Jaafar J., Lau W. J. and Matsuura T. Polysulfone/hydrous ferric oxide ultrafiltration mixed matrix membrane: Preparation, characterization and its adsorptive removal of lead (II) from aqueous solution. *Chemical Engineering Journal*. 2015 (289) 28–37.
169. Zhu M., Wang Y., Meng D., Qin X. and Diao G. Hydrothermal Synthesis of Hematite Nanoparticles and Their Electrochemical Properties. *Journal of Physical Chemistry C*. 2012 (116) 16276–16285.
170. Weiser H. B. and Milligan W. O. Von Weimarn's Precipitation Theory and the Formation of Colloidal Gold *Journal of Physical Chemistry*. 1931 (36) 1950–1959.
171. Zhong Z., Li D., Zhang B., and Xing W. Membrane surface roughness characterization and its influence on ultrafine particle adhesion. *Separation and Purification Technology*. 2012 (90) 140–146.
172. Su M., He C. and Shih K. Facile synthesis of morphology and size-controlled α -Fe₂O₃ and Fe₃O₄ nano- and microstructures by hydrothermal/solvothermal process: The roles of reaction medium and urea dose. *Ceramics International*. 2016 (42) 14793–14804.
173. Mohammadikish M. Hydrothermal synthesis, characterization and optical properties of ellipsoid shape α -Fe₂O₃ nanocrystals. *Ceramics International*. 2014 (40) 1351–1358.
174. Lu D., Zhang T., Gutierrez L., Ma J. and Croué J. P. Influence of Surface Properties of Filtration-Layer Metal Oxide on Ceramic Membrane Fouling during Ultrafiltration of Oil/Water Emulsion. *Environmental Science & Technology*. 2016 (50) 4668–4674.
175. Mahdavi H. R., Arzani M. and Mohammadi T. Synthesis, characterization and performance evaluation of an optimized ceramic membrane with physical separation and photocatalytic degradation capabilities. *Ceramics International*. 2018 (44) 10281–10292.
176. Chang Q., Zhou J., Wang Y., Liang J., Zhang X., Cerneaux S., Wang X., Zhu Z. and Dong Y. Application of ceramic microfiltration membrane modified by nano-TiO₂ coating in separation of a stable oil-in-water emulsion. *Journal of Membrane Science*. 2014 (456) 128–133.

177. Suresh K., Srinu T., Ghoshal A. K. and Pugazhenti G. Preparation and characterization of TiO₂ and γ -Al₂O₃ composite membranes for the separation of oil-in-water emulsions. *RSC Advances*. 2016 (6) 4877–4888.
178. Zhong Z., Xing W. and Zhang B. Fabrication of ceramic membranes with controllable surface roughness and their applications in oil/water separation. *Ceramics International*. 2013 (39) 4355–4361.
179. Chen X., Gao X., Fu K., Qiu M., Xiong F., Ding D., Cui Z., Wang Z., Fan Y. and Drioli E. Tubular hydrophobic ceramic membrane with asymmetric structure for water desalination via vacuum membrane distillation process. *Desalination*. 2018 (443) 212–220.
180. Babiker D. M. D., Zhu L., Yagoub H., Lin F., Altam A. A., Liang S., Jin Y. and Yang S. The change from hydrophilicity to hydrophobicity of HEC/PAA complex membrane for water-in-oil emulsion separation: Thermal versus chemical treatment,” *Carbohydrate Polymer*. 2020 (241) 116343.

LIST OF PUBLICATIONS

Journal with Impact Factor

1. **Syafikah Huda Paiman**, Mukhlis A Rahman, Tetsuo Uchikoshi, Norfadhilatuladha Abdullah, Mohd Hafiz Dzarfan Othman, Juhana Jaafar, Khairul Hamimah Abas and Ahmad Fauzi Ismail (2020). Functionalization effect of Fe-type MOF for methylene blue adsorption. *Journal of Saudi Chemical Society*, 24, 896–905. <https://doi.org/10.1016/j.jscs.2020.09.006>. **(Q2, IF: 3.517)**.
2. **Syafikah Huda Paiman**, Mukhlis A Rahman, Tetsuo Uchikoshi, Nik Abdul Hadi Md Nordin, Nur Hashimah Alias, Norfadhituladha Abdullah, Khairul Hamimah Abas, Mohd Hafiz Dzarfan Othman, Juhana Jaafar and Ahmad Fauzi Ismail (2020). In situ growth of α -Fe₂O₃ on Al₂O₃/YSZ Hollow Fiber Membrane for Oily Wastewater. *Separation and Purification Technology*, 23, 115250. <https://doi.org/10.1016/j.seppur.2019.116250>. **(Q1, IF: 5.774)**.
3. **Syafikah Huda Paiman**, Mukhlis A Rahman, Khairul Hamimah Abas, Azian Abd Aziz, Ahmad Fauzi Ismail, Mohd Hafiz Dzarfan Othman, Juhana Jaafar, Mohammad Noorul Anam Mohd Norddin (2019). Al₂O₃/YSZ Hollow Fiber Membrane Incorporated with Iron Oxide for Pb (II) Removal. *Chemical Engineering & Technology*, 42, 1321–1329. <https://doi.org/10.1002/ceat.201800065>. **(Q2, IF: 3.742)**.
4. Nur Hashimah Alias, Juhana Jaafar, Sadaki Samitsu, T Matsuura, AF Ismail, MHD Othman, Mukhlis A Rahman, Nur Hidayati Othman, Norfazliana Abdullah, **Syafikah Huda Paiman**, N Yusof, F Aziz (2018). Photocatalytic nanofiber-coated alumina hollow fiber membranes for highly efficient oilfield produced water treatment. *Chemical Engineering Journal*, 360, 1437–1446. <https://doi.org/10.1016/j.cej.2018.10.217>. **(Q1, IF: 10.652)**.

5. Nur Zhatul Shima Yahaya, **Syafikah Huda Paiman**, Norfazliana Abdullah, Nizar Mu'ammar Mahpoz, Amirul Afiat Raffi, Mukhlis A.Rahman, Khairul Hamimah Abbas, Azian Abd Aziz, Mohd Hafiz Dzarfan Othman, Juhana Jaafar (2019). Synthesis and characterization of MIL-140B-Al₂O₃/YSZ ceramic membrane using solvothermal method for seawater desalination. *Journal of the Australian Ceramic Society* 56, 291–300. DOI:10.1007/s41779-019-00435-2. (**Q2, IF: 1.307**).